Dynamic Redirection for Safe Interaction with ETHD-Simulated Virtual Objects

Yuqi Zhou, Voicu Popescu

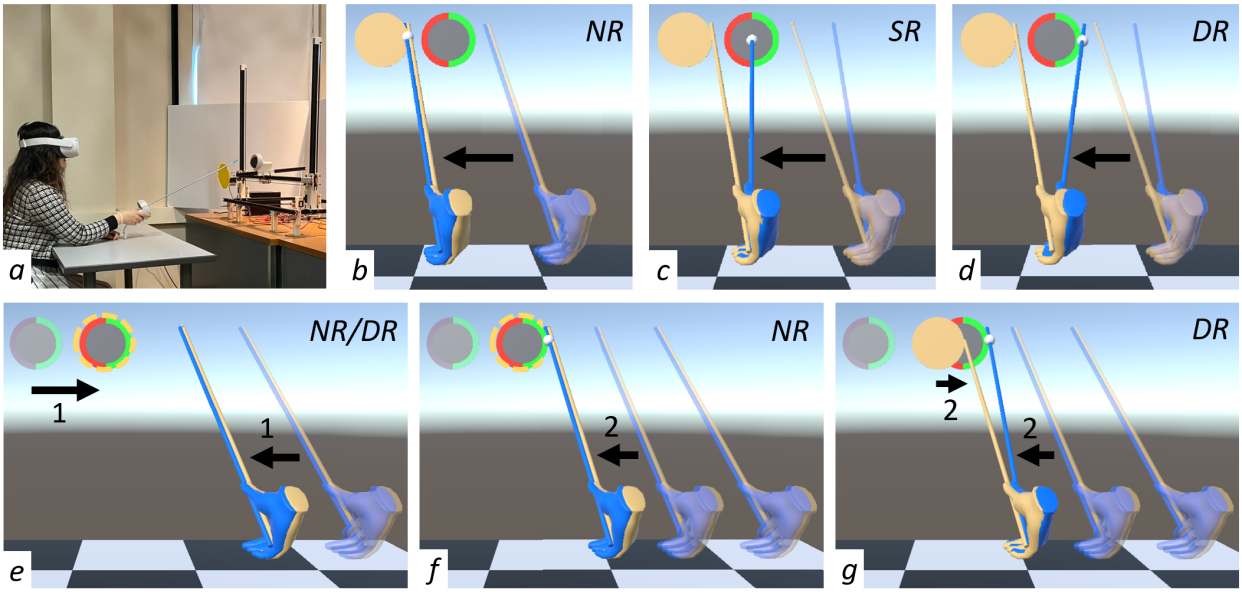

Fig. 1: Our custom $300 encountered-type haptic device (ETHD, *a*) and two experiments (*b-d* and *e-g*) conducted to evaluate our redirection strategy. The user taps a virtual disk and the ETHD carries a physical disk to provide haptic feedback. Images *b-g* are user frames from the VR headset, showing the virtual disk (red/green edge), and the virtual stick and user hand (blue). Here, the images also show the physical disk and user hand (brown), for illustration purposes. For experiment 1, by the time the physical stick hits the physical disk, the virtual stick slices through the virtual disk (*b*) with no redirection (NR), it enters the virtual disk (*c*) with static redirection (SR), and it stops correctly at the virtual disk's edge (*d*) with our dynamic redirection (DR). For experiment 2, the virtual disk is moving from left to right and the ETHD follows along; when the physical stick gets close to the physical disk, the ETHD stops, to enforce safety (*e*). For NR, the virtual disk stops as well (*f*), and the user notices that it stopped early, before contact. For DR, the virtual disk continues to move and our redirection algorithm synchronizes the virtual and physical contacts (*g*).

Abstract— This paper proposes a redirection strategy for safe and effective haptic feedback in virtual reality. The user interacts with the virtual environment using a handheld stick and receives haptic feedback from a custom $300 table-top encountered-type haptic device (ETHD). Safety is enforced by avoiding that the user makes contact with the ETHD while the ETHD is moving. Effectiveness is achieved by making sure users feel the physical contact at the same time as they see the contact in the virtual world. The haptic feedback strategy was evaluated in a controlled, within-subject user study (N = 26) with two experiments involving static and moving virtual objects. The results show that dynamic redirection of the virtual stick can satisfy simultaneously the competing goals of safety and effectiveness. Dynamic redirection has a significant advantage over no redirection and over static redirection both in terms of objective and subjective metrics.

Index Terms—Encountered-type haptic device, ETHD, redirection, VR haptics.

1 Introduction

Virtual reality (VR) can provide its users with a convincing immersive visualization of a 3D virtual environment. Allowing the user to not just see but also touch the objects in the virtual environment is challenging. One approach is passive haptic feedback, which relies on real world objects aligned with the virtual objects with which the user makes contact [25, 41]. Unfortunately, opportunities for passive haptic feedback are rather scarce, as it is unlikely that the real world happens to match the virtual environment closely. One option is to devise versatile physical props that can serve as convincing surrogates for many virtual objects [21, 22]. Another option is to rely on redirection to bridge the gap between misaligned virtual and physical objects [42]. A third option is to move a physical object at the encounter of the virtual object with which the user is going to make contact. This approach relies on an automated mechanical positioning system to carry an object at the anticipated contact point. The challenges with such encountered type haptic devices (ETHDs) include high equipment cost, and limited payload, speed, and range of motion [18, 26]. Another challenge is to ensure the user's safety by avoiding collisions with the invisible moving ETHD.

In this paper we propose a redirection strategy for safe and effective haptic feedback in VR. The user interacts with the virtual environment

- *Yuqi Zhou is with Purdue University. E-mail: zhou1168@purdue.edu.*
- *Voicu Popescu is with Purdue University. E-mail: popescu@purdue.edu.*

Manuscript received xx xxx. 201x; accepted xx xxx. 201x. Date of Publication xx xxx. 201x; date of current version xx xxx. 201x. For information on obtaining reprints of this article, please send e-mail to: reprints@ieee.org. Digital Object Identifier: xx.xxxx/TVCG.201x.xxxxxxx

using a handheld stick and receives haptic feedback from our custom $300 table-top ETHD. The ETHD is a Cartesian robot covering a 60 cm × 60 cm × 40 cm volume (Fig. 1*a*). Safety is enforced in two ways. First, the user doesn't touch the ETHD directly with their hand. Second, the ETHD stops when the stick gets close to the ETHD, so the user cannot make contact with the ETHD while the ETHD is moving. Effectiveness is achieved by synchronizing the visual contact between the virtual stick and the virtual object, and the mechanical contact contact between the physical stick and the physical object. Thereby, the user feels the physical contact at the same time as they see the contact in the virtual world. Our redirection strategy supports both stationary and dynamic virtual objects.

In addition to the safety benefit, having the user interact with the virtual environment through the handheld stick has the advantage of dulling the user's sense of touch, making the haptic feedback more believable than if it were imparted through the user's fingers [10, 22]. Indeed, when the user touches an object with their fingers they perceive many object properties such as texture and temperature. Any discrepancy with the expected properties of the virtual object will reduce the effectiveness of the haptic feedback. Another benefit of using the handheld stick is that the user is less aware of the position of the tip of the stick as they are of their fingers, which widens the design space and applicability of haptic redirection. Finally, there are many VR applications that call upon the user to interact with the virtual environment through a handheld tool, where our study of haptic feedback through the handheld stick has direct application.

The ETHD setup and dynamic redirection technique are ideal for scenarios requiring precise and safe physical-virtual interactions, such as surgical simulations or educational applications like virtual science laboratories. The system excels in controlled environments with moderate object velocities and precision demands. This work advances the ETHD field by enabling safer, more efficient dynamic haptic feedback, towards broader adoption in the VR community.

Our haptic feedback strategy was evaluated in an IRB-approved user study (N = 26) with two experiments. In one experiment participants were asked to tap a *stationary* virtual object with the handheld stick. The ETHD moves to assume the position of the virtual object in order to provide haptic feedback. When the stick gets close to the ETHD, the ETHD stops to enforce safety, leaving a gap between the ETHD and the virtual object. In one control condition (NR), no redirection is applied, and the virtual stick continues to travel through the virtual object until physical contact is made (Fig. 1*b*). In a second control condition (SR), a prior-art static redirection approach is used based on predicting the position of the ETHD relative the virtual object when contact is made; when the ETHD stops early of the predicted position, the virtual stick again intersects the virtual object (Fig. 1*c*). In the experimental condition (DR), the virtual stick is redirected using our strategy that takes into account the position of the ETHD in real time, so the virtual stick touches the edge of the virtual object as the physical stick touches the edge of the physical disk (Fig. 1*d*). The experiment measured the quality of the synchronization of visual and haptic feedback using both objective and subjective metrics. The results show that DR has a significant advantage over SR, and SR has a significant advantage over NR.

In a second experiment, participants were asked to stop a moving virtual object by tapping it from the direction opposite to its motion. At first, the ETHD moves in alignment with the virtual object (step 1 in Fig. 1*e*). When the stick gets close to the ETHD, the ETHD stops to enforce safety (end of step 1 in *e*). In the NR condition the virtual object stops with the ETHD, and the virtual stick continues to move in sync with the physical stick until contact is made (step 2 in *f*). Although the visual and haptic feedback are synchronized, the user might notice the early stop of the virtual object, and not as a consequence of being tapped. In the DR condition the virtual object continues to move after the ETHD stops, and the gap that forms between the physical and the virtual objects is bridged through dynamic redirection (step 2 in *g*). The results show that DR has a significant advantage over NR in conveying that the virtual object stopped when tapped by the user, and not earlier.

In summary, our paper contributes a low-cost table-top ETHD, a redirection approach for safe and effective haptic feedback in VR, and a user study validating the ETHD + redirection approach. We also refer the reader to the video accompanying our paper.

2 Related Work

We propose a passive haptic feedback approach using an ETHD and redirection. We briefly cover active haptic feedback approaches to focus on prior work with ETHDs, particularly safety strategies and haptic redirection in VR.

Active haptic feedback. One method for delivering haptic feedback involves users wearing haptic devices like gloves [2, 4], which apply pressure to their hands when interacting with virtual objects. This active approach allows mobility, making feedback accessible throughout the virtual environment. However, it has limitations, such as constant presence and unrealistic feedback, like pinching instead of genuine resistance. Solutions include a backpack-mounted robot arm to stop hand movement upon contact [18], though this increases encumbrance. Alternatively, non-contact methods, such as ultrasound, have been explored [31]. Ideal haptic feedback requires a physical object that mirrors the virtual one in shape, size, position, orientation, and surface properties. However, replicating the virtual world exactly is impractical. To overcome this, haptic feedback can either adapt the physical environment to match the virtual one or adjust the virtual world to fit the physical setting.

Encountered-type haptic devices (ETHDs). Researchers have long explored using robots to modify physical surroundings for haptic feedback. In 1993, McNeely introduced "robot graphics" [21], bridging visual and tactile perception in VR. Robots that move to simulate virtual objects are called "encountered-type haptic devices" (ETHDs). For a detailed overview, see a recent survey [25].

ETHDs vary in form. A typical ETHD is a robot arm [30], valued for its versatility, which can adapt to different applications by changing the attached object. For instance, a rolling prop with various textures can simulate different surfaces [20, 23]. However, the cost of robot arms increases significantly with reachability and payload. Solutions include adding rails to expand reachability [14] or using mobile platforms to carry the robot arm in larger spaces [26].

Our $300 ETHD balances affordability and functionality for consumer-level VR. Unlike higher-cost systems (e.g., $10,000+ robotic arms), it emphasizes accessibility while providing sufficient performance for tasks with limited payload and motion precision. This cost-effective design suits lightweight objects and controlled scenarios, such as VR training and simulations, making haptic technologies more accessible to research laboratories as well as consumer environments.

Researchers have also explored mobile robots for direct haptic feedback, offering simpler setups without robotic arms. For example, table-top robots provide strong downward pressure despite their small size [35]. Additionally, robots can rearrange physical objects to match virtual environments without holding them during interaction [34]. Ungrounded devices like drones can provide haptic feedback in large 3D spaces [9], although safety measures, such as caged propellers, are required to protect users.

ETHD safety strategies. Ensuring safety while maintaining effective haptic feedback presents conflicting constraints for ETHD motion [11]. The safest method when no feedback is required is to keep the ETHD at a safe distance from the user [26]. However, avoiding collisions without the user's awareness is not always feasible, especially when the ETHD lacks sufficient time to move away. To address this, researchers have combined covert safety mechanisms with overt approaches, such as informing users of potential collisions and enlisting their cooperation in avoidance [22]. A study exploring safety techniques for grounded robotic arms identified 18 methods, including revealing the ETHD or showing its trajectory [24]. Combining covert and overt techniques, such as keeping a drone outside the user's personal space while warning the user when necessary, has also been explored [7].

Our work complements existing methods for avoiding inadvertent collisions. Techniques such as visualizing the ETHD, switching to pass-through mode, or dodging can be applied to our ETHD. Our focus is on preventing collisions caused by the user's hand or tool

moving against the ETHD, which can result in high relative speeds and dangerous impacts. To address this, we implement a conservative safety protocol: stopping the ETHD when the user's stick gets close, ensuring any contact is with a stationary object. This protocol removes speed limitations for the ETHD, as it will always be stationary upon contact. Our contribution is hiding this early stopping from the user while preserving effective haptic feedback for dynamic virtual objects. To our knowledge, this is the first work to address safety for haptic feedback with *dynamic*, not just *static*, virtual objects.

Redirection. ETHDs modify the physical world to match the virtual one, while redirection adjusts the virtual world to align with the physical. Redirection techniques manipulate the virtual body, environment, or target object to synchronize virtual and physical contact, enabling convincing haptic feedback. Due to visual dominance, users prioritize what they see over what they feel, making small discrepancies between virtual and physical worlds imperceptible [12].

Redirection has proven effective for interacting with static objects [10], simulating large scenes with minimal setups [13], and even creating illusions of stiffness [37] or shape changes [6, 40]. It has also been used to simulate water resistance by restricting arm speed in a virtual environment [19]. Redirection is particularly effective when users interact with the virtual world using a handheld prop, as users are less aware of the prop's position than their own hand. For example, users were convinced they were hammering a nail into a plank, even when no nail was present [33]. Large redirection thresholds have been confirmed with handheld sticks, enabling both positional and shape redirection of target objects [42]. Redirection can extend the capabilities of ETHDs, such as increasing their reachability or reducing cost. It has been successfully combined with drones [7] and table-top mobile ETHDs, where the device moves ahead to meet the user's predicted target for synchronized contact [17].

Our approach combines ETHDs with redirection to provide safe and synchronized haptic feedback.

3 A Consumer-Level Table-Top ETHD

We implemented our ETHD using a table-top Cartesian robot assembled from off-the-shelf and 3D-printed PLA components (Fig. 2). The robot moves in three dimensions: one motor controls the x-axis (left-right), two motors control the y-axis (up-down), and two motors control the z-axis (near-far). The z-axis motors rotate a linear screw that moves the rails and y-axis motors, while the y-axis motors drive a belt that moves the x-axis. The belt on the y-axis is faster than the screw since it handles less weight. The x-axis also uses a belt to move the payload, which is a 14 cm diameter PLA disk providing haptic feedback. All five Nema 17 stepper motors (17HS4401S) are driven by A4988 drivers, mounted on a CNC shield V3 [1] and connected to an Arduino Uno [8]. The control board communicates with a laptop via USB, while the laptop and VR headset communicate wirelessly.

Calibration. To provide haptic feedback, the ETHD's coordinate system must be registered with the virtual environment's coordinate system. This automatic, one-time calibration per session requires no user input. The ETHD assumes four positions: an initial position I and three positions T_x, T_y, and T_z translated along the three axes. Using the VR controller carried by the ETHD, these positions are registered to the virtual environment when the controller remains stable for 4 seconds. Stability is defined as the controller staying within 1 cm of a position for 4 seconds. Calibration takes 20 seconds, largely due to confirming stability. The calibration accuracy, tied to the VR controller's tracking accuracy (4 ± 3 mm for Meta Quest 2 [28]), is sufficient for quality haptic feedback and much smaller than the redirection distances described in Sec. 5.

Tracking during use. After calibration, the ETHD is tracked using its stepping motors, which have high accuracy. Testing on an optical bench with a dial indicator shows the ETHD's positional accuracy to be 0.02 mm, far better than the Quest 2 controller's 1 mm tracking accuracy [29].

Versatility. The ETHD operates within a 60 cm $\times$ 60 cm $\times$ 40 cm volume, with speeds ranging from 10 cm/s to 22 cm/s on the x and y axes (belt mechanism) and 3 cm/s to 5 cm/s on the z axis (lead screw mechanism). It accelerates and stops quickly. The ETHD is invisible in the virtual environment, but its noise is noticeable, especially at slower speeds. It typically carries lightweight objects, though it conveys a large perceived weight when tapped with a user's stick due to its firm anchoring.

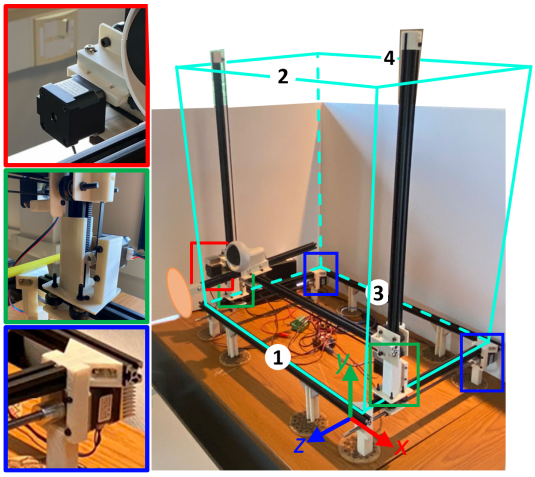

Fig. 2: Our ETHD that can position a physical object anywhere within a 60 cm x 60 cm x 40 cm region. The x (red), y (green), and z (blue) axis motion is implemented with two, two, and one stepper motor. The numbers indicate the four positions used in experiment 1.

The ETHD's design emphasizes simplicity and cost-effectiveness through off-the-shelf components and a Cartesian design, resulting in a compact, lightweight device providing safe haptic feedback within a 60 cm $\times$ 60 cm $\times$ 40 cm workspace. While alternatives like robotic arms offer greater precision and payload, they come with higher cost and complexity. Our ETHD delivers adequate performance for interactive VR tasks and remains accessible for broader applications, such as education and gaming.

A limitation of the current ETHD design is motor noise at lower speeds, which may reduce immersion in quiet environments. Mitigation approaches include quieter motor drivers, vibration-damping materials, or noise-cancellation algorithms integrated with the VR headset, enabling seamless operation in noise-sensitive settings.

4 Virtual Stick Redirection

While ETHDs modify the physical environment, another key approach for enhancing passive haptic feedback is to modify the virtual world through redirection. In our context, virtual stick redirection must address several considerations:

Synchrony. The primary goal is to synchronize virtual and physical contact to ensure believable haptic feedback.

Continuity. Redirection should occur seamlessly, avoiding abrupt changes in position, orientation, or scale, which could disrupt the user experience.

Relativity. Redirection should modify the user's motion as a gain, adjusting the virtual stick relative to the physical stick's movement. It should avoid moving the virtual stick when the physical stick is stationary or in a substantially different direction, as this would confuse the user.

The experiments compare dynamic redirection (DR) to no redirection and a prior static redirection (SR) method [17]. All techniques predict the contact points between the physical and virtual sticks and disks: S_p and O_p for the physical, and S_v and O_v for the virtual. The contact point estimation process is explained below.

Once these points are determined, the virtual stick is redirected as follows: the user-gripped end remains fixed, the direction is set by S_v, and the stick's length is adjusted so the tip's z-coordinate matches that of the physical stick. This approach focuses the redirection on the far end of the stick instead of altering the user's hand position, where users are less likely to notice the adjustments.

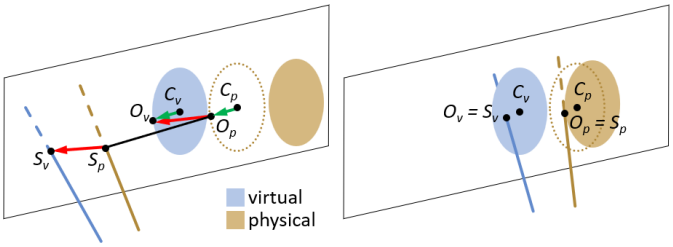

Fig. 3: Static redirection: approach (left) and problem of virtual stick intersecting virtual disk (right).

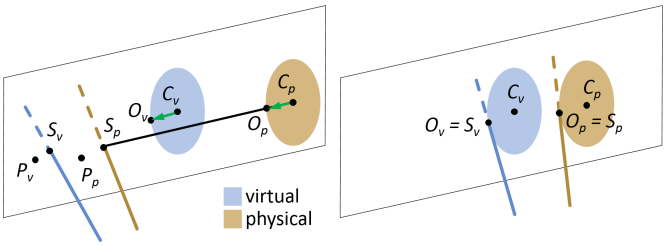

Fig. 4: Dynamic redirection: during swing (left) and virtual contact synchronized with physical contact (right).

4.1 No Redirection

One option is to ignore the misalignment between the physical and the virtual object. When the misalignment is large, the user is likely to notice the lack of synchrony, i.e., the user will see the virtual contact at a different time from when they feel the physical contact. This is particularly troublesome when the physical contact also serves the purpose of stopping the object with which the user interacts with the virtual object, i.e., the stick in our case. The lack of synchrony can lead to the virtual stick stopping early, before the virtual disk, or late, after intersecting the virtual disk.

4.2 Static redirection

A commonly used approach is to predict the relative position between the physical and virtual objects at the beginning of the redirection phase, and then to redirect over the subsequent frames based on this prediction [17]. This static redirection (SR) approach is illustrated in Fig. 3. When redirection begins, the position of the physical disk (dotted ellipse) is predicted for the moment when the virtual stick makes contact with the virtual disk.

The left panel shows the computation of the four contact points. The physical disk intersects the plane of the predicted physical disk at S_p. The **physical contact points** are computed as follows. O_p is set to the intersection between the line C_pS_p and the contour of the predicted physical disk, where C_p is the center of the predicted physical disk. If the physical disk does not intersect the plane, S_p is set to the tip of the stick, and O_p is computed using the projection of S_p onto the plane instead of S_p. The **virtual contact points** are computed as follows. O_v is computed with Eq. 1, which places O_v on the virtual disk at the same relative position of O_p on the predicted physical disk (green translation vectors in Fig. 3, left).

$$O_v = C_v + O_p - C_p \tag{1}$$

Finally, S_v is set gradually to a relative position from S_p that is the same as the relative position between O_v and O_p, as shown in Eq. 2. z_0 is the depth of a plane parallel to the disks and closer to the user (i.e., we use $z_0 = O_p.z + 1m$). At the beginning of redirection, When the tip S_p of the physical stick intersects with the z_0 plane, S_v starts to move away from S_p. When the tip of the physical stick intersects the plane of the disks, S_v has assumed its relative position to S_p given by $O_v - O_p$. Fig. 3, left, shows the case when the physical stick already intersects the plane, so $S_p.z = O_p.z$, and $S_v = S_p + (O_v - O_p)$.

$$S_v = S_p + (O_v - O_p) * max(0, (z_0 - S_p.z)/(z_0 - O_p.z)) \tag{2}$$

The static redirection satisfies the continuity requirement, as the predirected position is approached gradually. Static redirection also satisfies the relativity requirement. Consider the case when the user does not move the physical stick and the virtual disk does not move. In this case, even if the physical disk moves, its position predicted with respect to the virtual disk does not move, so all terms in the right hand side of Eq. 2 remain constant and the virtual stick does not move. Consider the case when the user does not move the physical stick and the virtual disk *does* move. In this case, the predicted position moves with the virtual disk, so $O_v - O_p$ and the virtual stick again does not move.

However, static redirection violates the synchrony requirement when the prediction turns out to be inaccurate. Fig.3, right, shows the scenario where the physical disk does reach the predicted position in time. The physical stick hits the contour of the physical disk, thus S_p is at the same position as O_p. According to Eq.1, O_v is within the virtual disk because O_p lies within the disk at the predicted position of the physical disk. Therefore, referring to Eq. 2, S_v is at the same position as O_v, so S_v also lies within the virtual disk. Consequently, the virtual stick intersects the virtual disk and is inside the virtual disk when the contact with the physical disk is made, thereby violating the synchrony requirement.

4.3 Dynamic redirection

We extend prior work on dynamic redirection [7,42] to support moving virtual and physical objects. Our approach is illustrated in Fig. 4. In the left panel, the physical contact points are computed like for the static redirection approach, except that we use the actual, and not the predicted, position of the physical disk. Then, like before, O_v is defined at the same relative position on the virtual disk contour as O_p on the contour of the physical disk (green translation vectors). What remains to be computed is the virtual stick contact point S_v that defines the redirection of the stick.

A naive solution for satisfying the synchrony requirement would be to keep the distance between the virtual stick and the virtual disk the same as that between the physical stick and the physical disk, i.e., $S_v - O_v = S_p - O_p$. This way when the distance between the physical stick and disk decreases to zero, so does the distance between the virtual stick and disk, synchronizing the contacts. However, this naive approach does not satisfy the relativity requirement. Consider the scenario when the user does not move the stick, or moves it very little. If the ETHD races to position the physical disk, the distance between the physical stick and disk changes, which requires changing the distance between the virtual stick and disk. Consequently, the virtual stick will have to move substantially, in a way that is saliently incongruent way with the motion that the user imparts to the stick. With such a naive approach the user would feel that the stick is radio controlled by a third party, making the redirection egregiously obvious.

To satisfy the relativity requirement alongside the synchrony and continuity requirement, we compute the virtual stick contact point S_v, without prediction, leveraging only the previous frame contact points, according to Algorithm 1.

The three coordinates of S_v are calculated independently (line 1). For most frames, while the stick moves and contact is not imminent, the control path takes line 7, which tunes the speed of the virtual disk to that of the physical disk; the velocities are computed using the previous stick contact points P_v and P_p. When the stick does not move, velocities cannot be estimated, and the exception is detected using line 2 and addressed using line 3, by keeping S_v unchanged. The case of imminent contact is detected by line 4, and handled by line 5, which sets the S_v at the same position on the virtual disk as S_p is on the physical disk. This case glues the virtual stick to the virtual disk and avoids small oscillations around the contact point. In practice we detect imminent contact with a θ value of 2 cm. Like for static redirection, to avoid a sudden jump once redirection begins, the effect of redirection

Algorithm 1 Virtual stick contact point update

Input: physical and virtual object centers C_p and C_v; physical and virtual object contact points O_p, and O_v, physical stick contact point S_p, previous frame virtual and physical stick contact points P_v and P_p
Output: virtual stick contact point S_v

1: **for** i ∈ {x, y, z} of S_v **do**
2: **if** $P_p.i = O_p.i$ **then**
3: $S_v.i = P_v.i$
4: **else if** $|O_p.i - P_p.i| < |O_p.i - S_p.i| < \theta$ **then**
5: $S_v.i = C_v.i + S_p.i - C_p.i$
6: **else**
7: $S_v.i = P_v.i + (O_v.i - P_v.i) * (S_p.i - P_p.i)/(O_p.i - P_p.i)$
8: $S_v = S_p + (S_v - S_p) * max(0, (z_0 - S_p.z)/(z_0 - O_p.z))$
9: **return** S_v

is gradually applied beyond an initial depth z_0 (line 8). In practice, we use a $z_0 = O_p.z + 1m$.

The algorithm achieves synchrony (Fig. 4, right) because when the physical stick gets close to the physical disk, so does the virtual stick to the virtual disk. In line 7 of Algorithm 1, as S_p approaches O_p, the ratio $(S_p.i - P_p.i)/(O_p.i - P_p.i)$ becomes 1 and S_v becomes O_v. Relativity is enforced because if the physical stick does not move, line 7 keeps S_v at its previous value P_v. Continuity is enforced by moving the virtual stick from frame to frame an amount commensurate with how much the physical stick moves.

Redirection has been extensively studied, with techniques ranging from static alignment, where physical and virtual objects are pre-aligned or whose alignment is predicted [10,17], to dynamic redirection, where alignment is continually adjusted in real time [42,43]. While static redirection is simpler to implement, it often results in noticeable misalignment artifacts, disrupting immersion during VR interactions. In contrast, dynamic redirection avoids these artifacts by maintaining precise alignment, even during complex interactions.

5 Evaluation

We have conducted an user study (approved by Purdue University Human Research Protection Program) to evaluate our approach's ability to convey haptic feedback through an ETHD in a way that is safe and effective. The user study compares dynamic redirection (DR) to no redirection (NR) and to static redirection (SR).

A first experiment (Experiment 1) investigated tapping a *static* virtual object, whereas in the second experiment (Experiment 2) the virtual object was *dynamic*.

Participants. We recruited 26 participants with the following demographics: the age range was 22 to 31 years, with an average of 27.2. Eight participants were women. One participant had never used a VR application before, two had used it once, 19 occasionally, and four frequently. All but one participant were right-handed. Due to this strong asymmetry, we excluded the data of the left-handed participant to avoid a confounding factor. This exclusion does not imply that the system is unsuitable for left-handed users.

The participant pool, limited to right-handed individuals aged 22 to 31, restricts the generalizability of our findings. Future studies should include left-handed participants and a broader age range, particularly older adults, to better assess the ETHD's potential in applications like motor rehabilitation and educational tools.

Participants provided consent and completed a demographic questionnaire before starting the experiments. Each participant completed two experiments in two sessions on separate days, with half starting with Experiment 1 and the other half with Experiment 2. Fatigue was considered, and the average completion time for Experiment 1 was 27.2 ± 2.99 minutes, while Experiment 2 took 18.2 ± 2.23 minutes.

Implementation and setup. We implemented the static and dynamic redirection methods in Unity3D (2022.3.4) [5], and the VR application was deployed on a Meta Quest 2 VR headset [3], as shown in Fig. 1. The participant was seated at an empty table 0.5 m wide that was placed directly against a second table holding the ETHD (Fig. 1*a*). The ETHD was described in Sec.3 (Fig. 2). The first table ensures that the participant can only touch the ETHD with the handheld stick and not directly with their hands. The physical disk was attached to the ETHD in a vertical position and in a way that gave the user access from all sides, free of collision with other parts of the ETHD. The participant was also asked to wear a pair of noise-canceling earbuds to avoid distractions from the real world, especially the noise from the motors.

5.1 Experiment 1: Static Virtual Object

The first experiment evaluates under what conditions the ETHD can convey haptic feedback safely and effectively to a user tapping a static virtual object. Safety requires that the ETHD stops before the user makes contact with it. Effectiveness requires synchronizing the visual and haptic feedback between the virtual stick and object.

Research hypotheses

RH1. In terms of quality of visual and haptic feedback synchronization, NR < SR < DR.

RH2. For NR and SR, the larger the gap between the virtual and physical objects, the lower the quality of visual and haptic feedback synchronization. For DR, the size of the gap does not affect the subjective quality of the synchronization.

Task. Participants are asked to tap the green edge of a virtual disk appearing in front of them (Fig. 1*b-d*). Due to virtual stick redirection, the visual contact between the virtual stick and disk may not align with the haptic feedback, causing the virtual stick to intersect the disk. Participants rate the synchronization by answering, "I made physical contact with the edge of the virtual disk," on a five-point Likert scale (1: Strongly disagree, 5: Strongly agree).

Conditions. The experiment uses a within-subject design, where all participants perform the task under all conditions. When the physical stick is within 10 cm of the physical disk, the ETHD stops to ensure safety. The three conditions differ in how the virtual disk is redirected to close the gap between the physical and virtual disks.

Additional Independent Variables. In addition to the three redirection conditions, the experiment explores two independent variables: (1) the position of the virtual disk at four different depths (30 cm range) and heights (50 cm range), as shown by labels 1-4 in Fig. 2; and (2) the speed of the ETHD, using three velocities: 12 cm/s, 16 cm/s, and 20 cm/s, sampling the ETHD's speed range.

Procedure. A trial involves a single tapping task, with the tap occurring within one second after the ETHD reaches the virtual disk (3.5s, 3s, and 2.5s for the three velocities). A timer above position 4 displays the remaining time, and exceeding the limit results in a trial repeat. A successful trial requires making *virtual* contact between the virtual stick and the green edge of the virtual disk, not *physical* contact. Occasionally, if the gap between the physical and virtual disks is too large and redirection is poor, the physical disk may be missed entirely. Each participant performed 12 practice trials followed by 108 trials (3 repetitions, 4 positions, 3 velocities, and 3 conditions).

Data collection (dependent variables). For each trial, we recorded the participant's subjective rating of the synchronization quality between visual and haptic feedback. We also measured the synchronization error objectively as the distance δ between the point where the virtual stick intersects the green edge of the virtual disk and the point where the virtual stick intersects the disk plane at the moment of physical contact (Fig. 1 *b-d*). A $\delta = 0$ indicates perfect synchronization between visual and haptic feedback. δ is undefined when no physical contact is made, and we report the number of trials where this occurred. Additionally, we recorded the distance ε between the virtual and physical disks when the physical disk stops, indicating the gap redirection needs to bridge.

Data analysis. We compared the synchronization quality between visual and haptic feedback across three conditions using participants' subjective ratings and the objective error δ. Since our within-subject data is not normally distributed, we applied the Friedman non-parametric test [16] for comparisons, followed by a Wilcoxon post-hoc pairwise

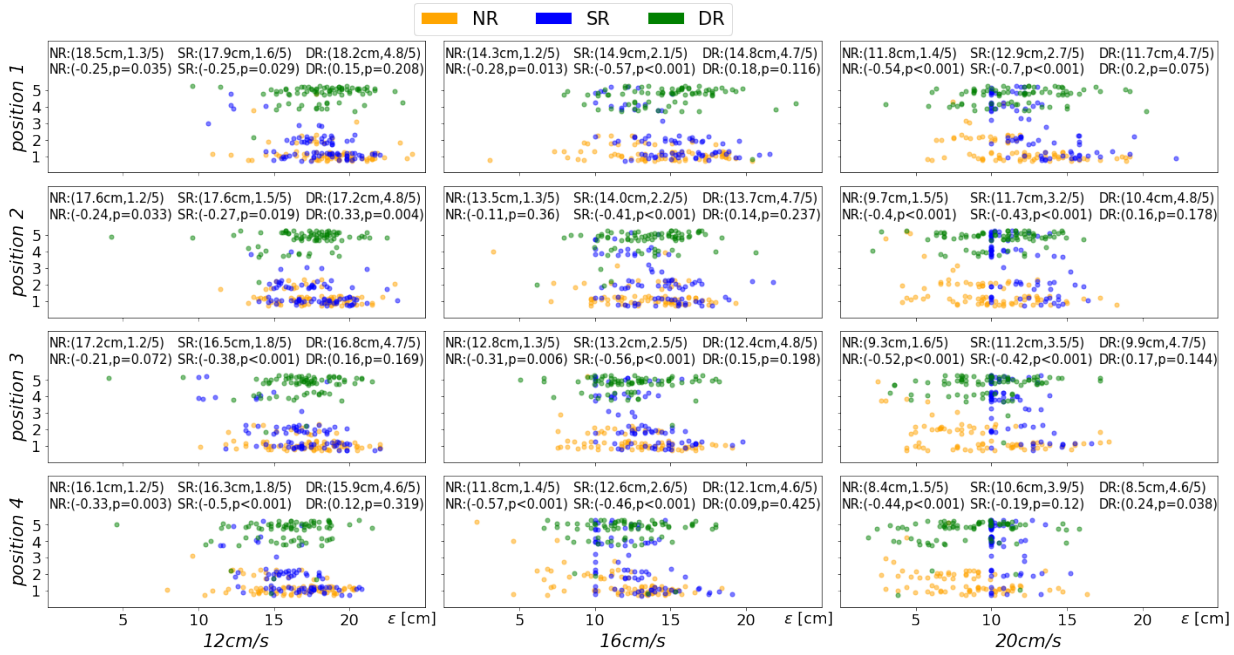

Fig. 5: Subjective rating of visual and haptic feedback synchronization, for each position (rows) and each ETHD speed (columns). Each scatter-plot panel has the gap ε between the virtual and physical disks on the x axis, and the rating on a five-point Likert scale as the y axis. Each panel shows the dots for the 25 participants, three repetitions, and three conditions, with cumulative transparency. At the top of each panel, the first row gives the average ε and average rating, for each condition; the second row gives Spearman's rank correlation between rating and ε.

analysis [38] with a Bonferroni correction ($\times 3$) for the three pairs of conditions.

Spearman's rank correlation coefficient [32] was used to assess correlations with the Likert-scale ratings, while Pearson's correlation coefficient was used for continuous variables δ and ε. All statistical analyses were conducted using the SciPy package [36].

Results and discussion.

RH1. Fig. 5 and Fig. 6 give the subjective synchronization quality for all positions, ETHD velocities, conditions, and participants. For each position / ETHD speed combination, there is a significant difference in terms of subjective rating between the three conditions (Friedman p values under 0.001 for each of the 12 panels). The post-hoc analysis shows that DR has a significant advantage over each of NR and SR (Wilcoxon's $p < 0.001$ for each of the 12 panels). Furthermore, SR has a significant advantage over NR (Wilcoxon's $p < 0.02$ for each of the 12 panels) supporting RH1.

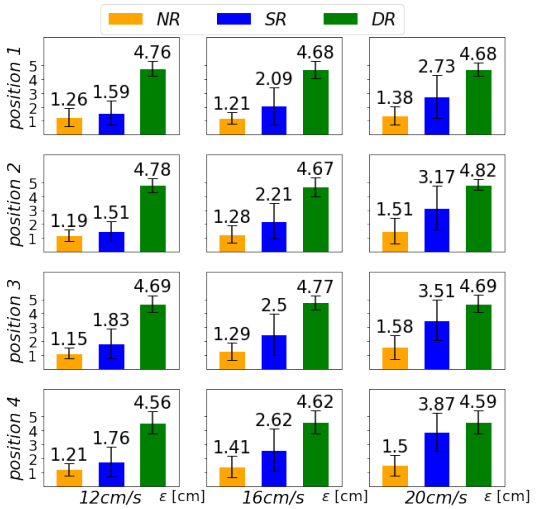

Fig. 6: Box plot visualization of subjective rating of visual and haptic feedback synchronization, for each position (rows) and each ETHD speed (columns).

Fig. 7 shows that the objective measure of the synchronization error δ is large for SR, even larger for NR, and virtually 0 for DR, for all positions, and for all ETHD velocities. Consequently, DR has a significant advantage over SR, and SR has a significant advantage over NR, with Friedman and Wilcoxon significance values $p < 0.001$, for each position/speed combination, confirming RH3. The only exception is for the pairwise comparison of DR over SR for the ETHD speed of 20 cm/s and position 4, where Wilcoxon's $p = 0.056$. In this case, the fast ETHD and the distant position 4 can provide enough time for the ETHD to reach the desired SR position. That is, RH1 is supported both subjectively and objectively.

RH2. Fig. 5 shows that the subjective rating is negatively correlated with ε for both NR and SR, i.e., Spearman $p < 0.05$ in the second row of the title of each panel, and that the subjective rating is not correlated with ε for DR, confirming RH2. We attribute the few exceptions (2 out of 12 for NR, 1 for SR, and 2 for DR) to ratings that are uniformly low or high, obscuring the correlation.

Fig. 7 shows that our results also support RH2 objectively. For NR, there is no redirection so the virtual stick remains aligned with the physical stick, which means that δ and ε are approximately equal in all cases. For SR, δ measures the residual distance between the goal of 10 cm and the actual ε value. In other words, δ starts at 0 cm for $\varepsilon = 10cm$ and then grows linearly with ε. For DR δ is 0 in all cases since dynamic redirection always closes the gap, but it is not exactly 0 due to virtual to physical registration errors and due to measurement latency errors. In conclusion, δ correlates with ε for NR and SR (significant Pearson's linear correlation), but not for DR. Thus, RH2 is supported both subjectively and objectively.

Haptic feedback miss rate. The physical stick trajectory is not always perfectly horizontal, so when the physical and virtual disks are severely misaligned and the redirection is poor, a participant can miss the physical disk altogether, receiving no haptic feedback at all. Fig. 7 (third row at top of each panel) shows that the larger the δ value,

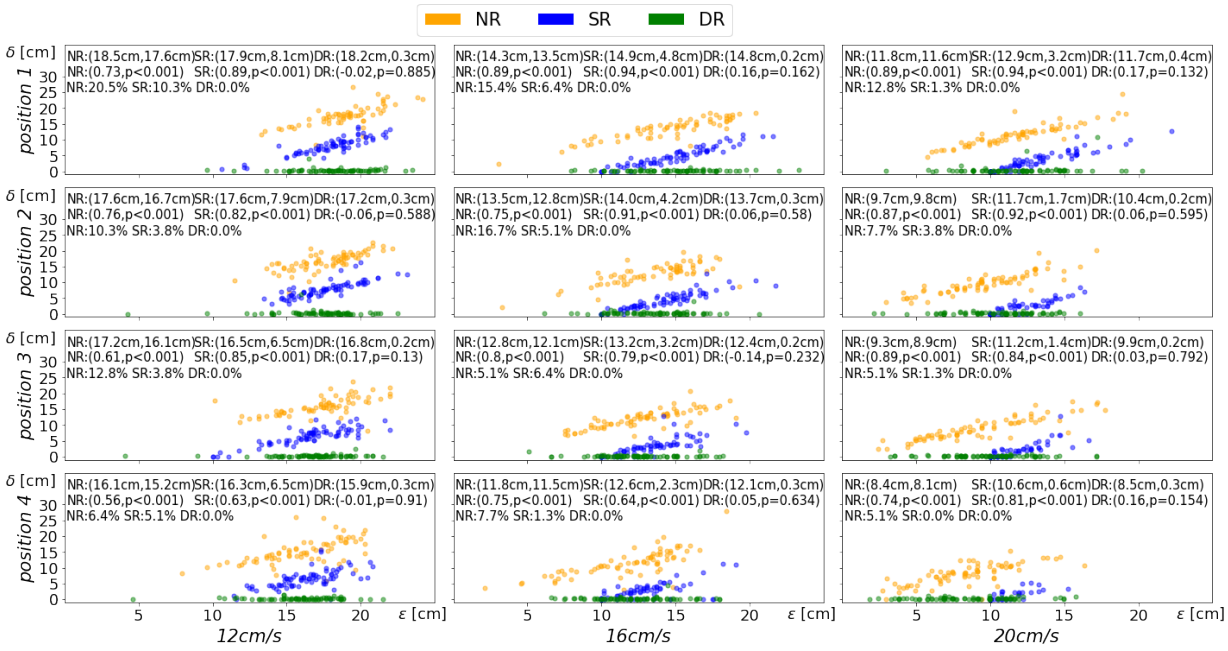

Fig. 7: Objective synchronization error δ, for each position (rows) and each ETHD speed (columns). Each scatter-plot panel has the gap ε on the x axis, and δ on the y axis. Each panel shows the dots for the 25 participants, three repetitions, and three conditions, with cumulative transparency. At the top of each panel, the first row gives the average ε and δ, for each condition; the second row gives the Pearson correlation between ε and δ; the third row gives the rate at which participants missed the physical disk (no haptic feedback).

the higher the miss rate. For DR, no participant has ever missed the physical disk, confirming the quality of the redirection.

5.2 Experiment 2: Dynamic Virtual Object

Whereas the first experiment examines interactions with static virtual objects, the second experiment evaluates the ability of our ETHD combined with redirection to provide haptic feedback during interactions with dynamic virtual objects. In this case, the ETHD must continuously move to keep pace with the virtual object, increasing safety concerns—likely a reason why prior research has largely avoided providing haptic feedback for moving objects. However, dynamic haptic feedback is crucial for applications like virtual laboratories, where users must interact with moving objects, as demonstrated in the "Towards Applications" segment of the supplemental video.

To ensure safety, we stop the ETHD when the user approaches it, and our dynamic redirection algorithm compensates for the gap between the moving virtual object and the stationary ETHD.

For safety reasons, the ETHD stops when the user is about to collide with it in the opposite direction of its motion. In the case of a moving virtual object, not using redirection (NR) will result in the virtual object stopping prematurely, before the user makes contact. This early stopping will be noticeable, breaking the illusion that the object stops due to the user's action. Dynamic redirection (DR), however, allows the virtual object to keep moving until contact is made, concealing the early stopping from the user.

The visibility of early stopping depends on how much earlier the virtual object halts before user contact, which is influenced by both the safety stopping distance and the user's speed. A longer stopping distance and slower user movement increase the time between the virtual object stopping and the user's contact. Based on this, we propose the following research hypotheses.

Research hypotheses.

RH3. Participants will notice that the virtual object stops before contact for NR, and not for DR.

RH4. For NR, the longer the delay between when the virtual object stops and when contact is made, the more noticeable the early stop. For DR there is no delay between stopping and contact.

Task and conditions. We designed a task to compare dynamic redirection (DR) with no redirection (NR) when interacting with a moving virtual object. Initially, the virtual and physical disks, as well as the virtual and physical sticks, are aligned and move together (Fig. 1*e*). When the physical stick approaches the physical disk, the ETHD stops for safety.

In the NR condition, the virtual disk stops as soon as the ETHD stops, keeping the virtual and physical disks synchronized. The virtual and physical sticks remain in sync until contact is made (Fig. 1*f*). In the DR condition, the virtual disk continues to move after the ETHD has stopped, creating a gap between the virtual and physical disks that is bridged through dynamic redirection (Fig. 1*g*). Both conditions maintain synchronized visual and haptic feedback, but in the NR condition, the virtual disk stops early, before the user makes contact. After tapping the virtual disk, participants were asked whether "the virtual disk stopped before [they] tapped it," with a yes/no response.

Additional Independent Variables. In addition to the two conditions above, the experiment investigated three additional independent variables. The first is the direction of the disk's movement, with three directions: left to right (RIGHT), right to left (LEFT), and top to bottom (DOWN). The second variable is the safety stopping distance, with three values: 10 cm, 15 cm, and 20 cm. The third variable is the ETHD speed, with two values: 12 cm/s and 20 cm/s. By exploring different safety stopping distances and speeds, we create a benchmark that can be applied to other ETHDs with varying velocities and stopping times.

Procedure. Each participant performed 18 practice trials followed by 108 counter-balanced actual trials.

A **trial** consisted of a single tapping task where the participant started from the same hand position, i.e. close to their shoulder. The physical disk started from one of three locations, depending on its moving direction. The disk could travel at most 30 cm, which means that the participant had to tap the disk in 1.5s or 2.5s, for the two velocities. The participant was shown the count down and needed to redo the trial if the time was exceeded. If the tap occurred within the allotted time, the participant was shown the question.

The **18 practice trials** familiarized the participant with the task. The participant was instructed to tap the virtual disk with a natural swinging motion. Although participants started out tentatively, they picked up

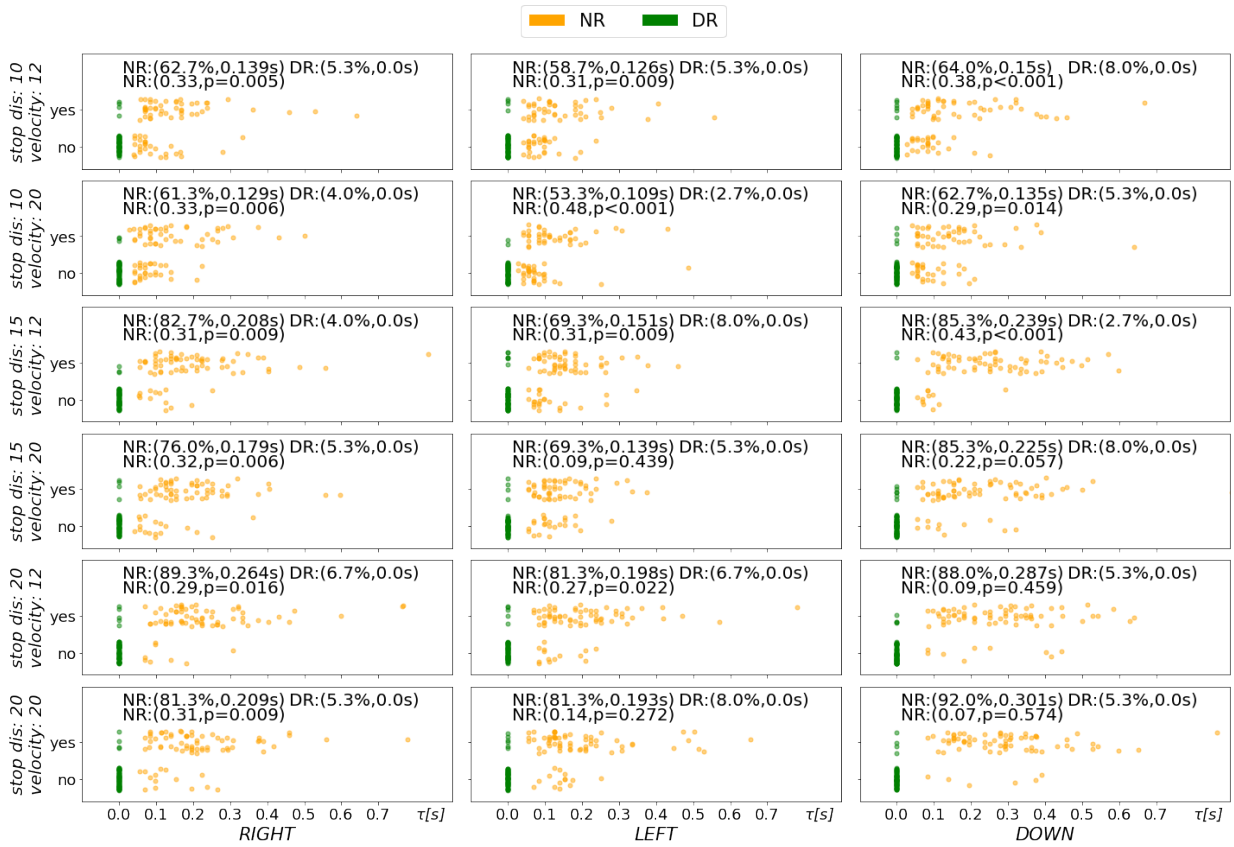

Fig. 8: Scatter plots of the yes/no answers to the early stopping detection question, for all 8 combinations of safety stopping distance and speed values (rows), and for all tapping directions (columns). Each plot has the delay τ on the x axis, and the binary answer on the y axis. Each plot shows 150 dots (25 participants, three repetitions, and two conditions) with cumulative transparency. At the top of each panel, the first row gives the percentage of yes answers and the average τ for each condition; the second row gives the point-biserial correlation coefficient [39] between the yes answers and τ.

the pace after the first few practice trials and were able to tap the disk within the allotted time. The noise cancelling earbuds prevented the participant from hearing whether the ETHD was stopped or moving. The practice trials used the three moving directions and the three safety stopping distances, for each of the two conditions, with an ETHD speed of 20 cm/s. The **108 experiment trials** repeated 3 times all speed (2), safety stopping distance (3) and direction (3) combinations, for each of each condition (2).

Data collection (dependent variables). For each trial, we recorded whether the participant noticed the early stopping of the virtual disk. In addition, we also recorded objectively the delay τ between when the virtual disk stopped and when contact was made.

Data analysis. We computed the percentage of yes's in the 75 answers (25 participants $\times$ 3 repetitions), for each speed, direction, and safety distance combination. We used the Chi-square test [27] to compare this binary variable across three directions, two velocities, and three safety stopping distances. When a significant difference was found, we used Fisher's exact test [15] for pairwise comparisons. The delay τ was compared across independent variables using Friedman's test followed by a Wilcoxon's posthoc analysis.

Results and discussion

RH3. Fig. 8 gives the early stopping detection rates. For NR, the percentage of yes answers is always above 50%, and for DR, it is always below 10%, which supports RH3.

RH4. For NR, the delay τ between when the virtual object stops and contact is made depends on the the safety stopping distance and on the swing speed. Leveraging the swing traces we investigated the swing speed, which was on average 1.18 m/s$\pm$0.63 m/s. In Fig. 8 the swing speed is reflected by the average delay τ for NR (e.g., 0.139s for the top left graph), which gives the time the physical stick needs to cover the safety stopping distance. Fig. 8 shows that the swing speed increases (i.e., τ decreases) when the virtual object (i.e., ETHD) speed changes from 12 cm/s to 20 cm/s, which is expected since participants have to hurry to make contact with the moving virtual object before the trial timer expires. However, these differences are no significant.

The dominant factor affecting τ is the safety stopping distance. There is a significant difference for τ between the three safety stopping distances (Friedman $p < 0.05$), for all combinations of three direction and two ETHD speed values. The Wilcoxon's pairwise posthoc analysis confirms significantly larger τ values for the larger safety stopping distance of each pair, with the $\times 3$ Bonferroni correction accounting for the three pairs of conditions. These objective measures of the early stopping are confirmed subjectively by the participants. Tab. 1 compares the early stopping detection rates for the three safety stopping distances. The longest safety stopping distance (20 cm) results in significantly larger detection rates than the shortest safety stopping distance (10 cm), for all six speed and direction combinations. There is never a significant difference between the safety stopping distances of 15 cm and 20 cm. In conclusion, the data supports RH4, with the caveat that the difference in safety stopping distance has to be sufficiently large (e.g., 10 cm vs 20 cm) for the difference in τ to impact the early detection rate.

The early stopping detection rate correlates significantly with τ in 13 out of the 18 plots in Fig. 8 (second row in title). The correlation breaks down for the larger safety stopping distances and the less natural tapping directions, i.e., in the bottom right corner of the matrix of plots. This occurs for high values of the early stopping detection rate, which is saturated and not sensitive anymore to τ.

speed	*safety stopping distance comparisons*	*RIGHT*	*LEFT*	*DOWN*
12 cm/s	*Chi-square*	p <0.001 χ^2 = 16.96	p = 0.008 χ^2 = 9.15	p <0.001 χ^2 = 15.71
	10 cm vs 15 cm	p = 0.03	p = 0.701	p = 0.013
	15 cm vs 20 cm	p = 1.041	p = 0.387	p = 2.432
	10 cm vs 20 cm	p <0.001	p = 0.012	p = 0.003
20 cm/s	*Chi-square*	p <0.027 χ^2 = 8.14	p = 0.003 χ^2 = 13.6	p <0.001 χ^2 = 22.17
	10 cm vs 15 cm	p = 0.233	p = 0.194	p = 0.008
	15 cm vs 20 cm	p = 1.651	p = 0.387	p = 0.909
	10 cm vs 20 cm	p = 0.033	p = 0.001	p <0.001

Table 1: Comparisons of early stopping detection rates between the three safety stopping distances, for each of the three directions and each of the two ETHD velocities, in the NR condition. All Chi-square tests reveal significant differences between the three safety stopping distances. The pairwise comparisons (Fisher's exact with a $\times 3$ Bonferroni correction) that are significant are shown in red, and not significant in black.

5.3 Summative discussion of the study results

Research hypothesis support. Overall, all six research hypotheses were supported by the experimental data. As DR achieves synchronization and avoids early stopping by design, this does not come at a surprise. The experimental results confirm that dynamic redirection algorithm has the prerequisite robustness over a wide range of parameters and parameter values for integration into VR applications. In relation to prior work that employs static redirection, our ETHD + dynamic redirection approach has the advantage of better synchronization, even when strictly enforcing a safety protocol. In other words, dynamic redirection is sufficiently supple to bridge virtual to physical gaps as required for safety. Our work has demonstrated the dynamic redirection qualities in the context of a single safety protocol, but future work could study dynamic redirection in conjunction with other safety protocols, as dictated by specific ETHDs and applications.

ETHD safety. A primary concern for our work is ETHD safety. In our context, ETHD safety does not mean *avoiding* collisions with the ETHD, but rather ensuring that these collisions are safe, i.e., that the user does not hit against a moving ETHD. Our safety concerns are orthogonal to those of prior work where the emphasis is on avoiding inadvertent collisions [24, 26]. The contribution of our work lies in respecting this simple and conservative safety protocol *without sacrificing the effectiveness* of the haptic feedback. Experiment 2 shows that our ETHD + dynamic redirection strategy successfully dissimulate the implementation of the safety protocol, preserving haptic feedback effectiveness. Our findings could be used in the future to allow potentially dangerous ETHDs to operate safely, using their full range of mechanical capabilities, to provide effective haptic feedback in a wide range of scenarios.

Generality of dynamic redirection. We have demonstrated the generality of our redirection algorithm in supporting various safety protocols and its adaptability to different ETHDs and interaction modalities. Although tested with a Cartesian robot, the algorithm is agnostic to robot design, relying solely on the poses of the manipulant (e.g., stick) and the carried object. Tasks like 3D object positioning could be performed by robotic arms or mobile robots. The Cartesian robot was chosen for its simplicity and cost-effectiveness, but the algorithm can generalize to more complex ETHDs with additional degrees of freedom. While extending to single-finger interactions is straightforward, tasks involving multiple fingers or grasping are beyond the current scope, as the algorithm assumes a single contact point. Operating independently of mechanical configurations, the algorithm uses inverse kinematics and non-linear optimizations to align the manipulant and virtual object. Future work will extend the algorithm to diverse ETHD designs and tasks to validate its robustness and versatility further.

Furthermore, Fitts' Law is relevant to our system, as the distances between the user's hand, virtual stick, and target affect task efficacy. Fitts' Law predicts increased difficulty with greater distances and smaller targets, aligning with physical-virtual alignment challenges in haptic systems. Our dynamic redirection technique mitigates these challenges by maintaining alignment and reducing perceived difficulty. Although this study did not explicitly analyze Fitts' Law, future work could explore its impact by varying target distances and sizes to better understand its role in task performance and haptic feedback perception.

6 Conclusions. Limitations. Future work

We have presented a redirection strategy for haptic feedback in VR that satisfies the conflicting goals of safety and realism. We have assembled an ETHD to evaluate our redirection strategy with static and dynamic virtual objects tapped by the user with a handheld stick. The redirection strategy provides well-synchronized visual and haptic feedback even for sizeable gaps between the ETHD and the virtual object, in both static and dynamic scenarios.

One limitation of this work is its reliance on a Cartesian robot, which offers a favorable reachability-to-cost ratio but restricts the carried object to three degrees of freedom, limiting haptic feedback to a single direction. Future work could explore compensating for this limitation with more complex carried object shapes, such as multi-headed designs, allowing redirection strategies to select the most suitable head for virtual contact. Additionally, research could investigate extending the ETHD's reachability in ways that remain undetectable or acceptable to users and applications, further enhancing its capabilities.

While our experiments focused on single-point tapping tasks, future work could evaluate more complex scenarios, such as interactions with multiple dynamic objects or multi-contact manipulation, to test the scalability and robustness of our dynamic redirection algorithm and validate its applicability to diverse VR environments.

Integrating dynamic redirection with direct hand interactions offers exciting opportunities but poses challenges, including multi-finger input, tactile feedback, and safety. While our current system uses handheld sticks for simplicity, hand interactions could enhance immersion by providing richer haptic feedback, requiring precise tracking and improved redirection algorithms for multiple contact points. Future work could explore combining our technique with tactile gloves or sensor-equipped ETHDs for seamless, natural interactions.

Even with perfect device tracking, our dynamic redirection technique remains essential. While precise tracking reduces positional discrepancies, it does not address challenges like synchronizing physical-virtual interactions during dynamic tasks or ensuring safety during rapid movements. For instance, unpredictable object motion requires real-time alignment adjustments. Additionally, dynamic redirection mitigates hardware limitations, such as actuator latency or motion deviations, ensuring seamless and safe haptic feedback even in ideal tracking conditions.

Our medium-term goal is to develop a table-top ETHD capable of safely and convincingly providing haptic feedback for single or multiple virtual objects, static or dynamic, to enhance immersive learning in virtual science, technology, and engineering laboratories. While our experiment involved stopping virtual objects upon contact to test early stopping detection, the approach is adaptable to other interactions, such as bouncing objects, as shown in the accompanying video. The young participant group in this study is suitable for virtual laboratory applications. Long-term, we aim to expand our approach to applications like motor skill rehabilitation, requiring studies with a broader range of ages and psycho-motor abilities.

Future enhancements to the ETHD system could include integrating sensory modalities like synchronized audio and visual feedback to enhance immersion. Spatial sound effects could signal proximity or collisions, while visual overlays might mask minor physical-virtual alignment discrepancies. Such modalities could improve the perception of dynamic redirection by creating a cohesive multisensory experience, reducing sensitivity to subtle inconsistencies.

Acknowledgments

This material is based upon work supported by the National Science Foundation under Grants No. 2212200 and 2309564.

REFERENCES

[1] Cnc shield v3. http://www.hiletgo.com/. Accessed: 2024-08-22. 3

[2] Haptx vr gloves. https://haptx.com/. Accessed: 2024-08-22. 2

[3] Oculus headset. https://www.oculus.com/. Accessed: 2024-08-22. 5

[4] touchdiver. https://www.weart.it/. Accessed: 2024-08-22. 2

[5] Unity 3d engine. https://unity.com/. Accessed: 2024-08-22. 5

[6] P. Abtahi and S. Follmer. Visuo-haptic illusions for improving the perceived performance of shape displays. In *Proceedings of the 2018 CHI Conference on Human Factors in Computing Systems*, pp. 1–13, 2018. 3

[7] P. Abtahi, B. Landry, J. Yang, M. Pavone, S. Follmer, and J. A. Landay. Beyond the force: Using quadcopters to appropriate objects and the environment for haptics in virtual reality. In *Proceedings of the 2019 CHI Conference on Human Factors in Computing Systems*, pp. 1–13, 2019. 2, 3, 4

[8] Arduino. Arduino - home. https://www.arduino.cc/. Accessed: 2024-08-22. 3

[9] M. I. Awan, A. Raza, and S. Jeon. Dronehaptics: Encountered-type haptic interface using dome-shaped drone for 3-dof force feedback. In *2023 20th International Conference on Ubiquitous Robots (UR)*, pp. 195–200. IEEE, 2023. 2

[10] M. Azmandian, M. Hancock, H. Benko, E. Ofek, and A. D. Wilson. Haptic retargeting: Dynamic repurposing of passive haptics for enhanced virtual reality experiences. In *Proceedings of the 2016 chi conference on human factors in computing systems*, pp. 1968–1979, 2016. 2, 3, 5

[11] E. Bouzbib and G. Bailly. " let's meet and work it out": Understanding and mitigating encountered-type of haptic devices failure modes in vr. In *2022 IEEE Conference on Virtual Reality and 3D User Interfaces (VR)*, pp. 360–369. IEEE, 2022. 2

[12] E. Burns, S. Razzaque, A. T. Panter, M. C. Whitton, M. R. McCallus, and F. P. Brooks Jr. The hand is more easily fooled than the eye: Users are more sensitive to visual interpenetration than to visual-proprioceptive discrepancy. *Presence: teleoperators & virtual environments*, 15(1):1–15, 2006. 3

[13] L.-P. Cheng, E. Ofek, C. Holz, H. Benko, and A. D. Wilson. Sparse haptic proxy: Touch feedback in virtual environments using a general passive prop. In *Proceedings of the 2017 CHI Conference on Human Factors in Computing Systems*, pp. 3718–3728, 2017. 3

[14] S. Dai, J. Smiley, T. Dwyer, B. Ens, and L. Besancon. Robohapalytics: a robot assisted haptic controller for immersive analytics. *IEEE Transactions on Visualization and Computer Graphics*, 29(1):451–461, 2022. 2

[15] R. A. Fisher. On the interpretation of χ 2 from contingency tables, and the calculation of p. *Journal of the royal statistical society*, 85(1):87–94, 1922. 8

[16] M. Friedman. The use of ranks to avoid the assumption of normality implicit in the analysis of variance. *Journal of the american statistical association*, 32(200):675–701, 1937. 5

[17] E. J. Gonzalez, P. Abtahi, and S. Follmer. Reach+ extending the reachability of encountered-type haptics devices through dynamic redirection in vr. In *Proceedings of the 33rd Annual ACM Symposium on User Interface Software and Technology*, pp. 236–248, 2020. 3, 4, 5

[18] A. Horie, M. Y. Saraiji, Z. Kashino, and M. Inami. Encounteredlimbs: A room-scale encountered-type haptic presentation using wearable robotic arms. In *2021 IEEE Virtual Reality and 3D User Interfaces (VR)*, pp. 260–269. IEEE, 2021. 1, 2

[19] H. Kang, G. Lee, and J. Han. Visual manipulation for underwater drag force perception in immersive virtual environments. In *2019 IEEE Conference on Virtual Reality and 3D User Interfaces (VR)*, pp. 38–46. IEEE, 2019. 3

[20] Y. Kim, S. Kim, U. Oh, and Y. J. Kim. Synthesizing the roughness of textured surfaces for an encountered-type haptic display using spatiotemporal encoding. *IEEE Transactions on Haptics*, 14(1):32–43, 2020. 2

[21] W. A. McNeely. Robotic graphics: a new approach to force feedback for virtual reality. In *Proceedings of IEEE Virtual Reality Annual International Symposium*, pp. 336–341. IEEE, 1993. 1, 2

[22] V. Mercado, M. Marchai, and A. Lécuyer. Design and evaluation of interaction techniques dedicated to integrate encountered-type haptic displays in virtual environments. In *2020 IEEE Conference on Virtual Reality and 3D User Interfaces (VR)*, pp. 230–238. IEEE, 2020. 1, 2

[23] V. Mercado, M. Marchal, and A. Lécuyer. Entropia: towards infinite surface haptic displays in virtual reality using encountered-type rotating props. *IEEE transactions on visualization and computer graphics*, 27(3):2237–2243, 2019. 2

[24] V. R. Mercado, F. Argelaguet, G. Casiez, and A. Lécuyer. Watch out for the robot! designing visual feedback safety techniques when interacting with encountered-type haptic displays. *Frontiers in Virtual Reality*, 3:928517, 2022. 2, 9

[25] V. R. Mercado, M. Marchal, and A. Lécuyer. "haptics on-demand": A survey on encountered-type haptic displays. *IEEE Transactions on Haptics*, 14(3):449–464, 2021. 1, 2

[26] S. Mortezapoor, K. Vasylevska, E. Vonach, and H. Kaufmann. Cobodeck: A large-scale haptic vr system using a collaborative mobile robot. In *2023 IEEE Conference Virtual Reality and 3D User Interfaces (VR)*, pp. 297–307. IEEE, 2023. 1, 2, 9

[27] K. Pearson. X. on the criterion that a given system of deviations from the probable in the case of a correlated system of variables is such that it can be reasonably supposed to have arisen from random sampling. *The London, Edinburgh, and Dublin Philosophical Magazine and Journal of Science*, 50(302):157–175, 1900. 8

[28] D. Pereira, V. Oliveira, J. L. Vilaça, V. Carvalho, and D. Duque. Measuring the precision of the oculus quest 2's handheld controllers. In *Actuators*, vol. 12, p. 257. MDPI, 2023. 3

[29] D. Pereira, V. Oliveira, J. L. Vilaça, V. Carvalho, and D. Duque. Measuring the precision of the oculus quest 2's handheld controllers. In *Actuators*, vol. 12, p. 257. MDPI, 2023. 3

[30] J. Posselt, L. Dominjon, A. Bouchet, and A. Kemeny. Toward virtual touch: Investigating encounter-type haptics for perceived quality assessment in the automotive industry. In *Proceedings of the 14th Annual EuroVR Conference, Laval, France*, pp. 12–14, 2017. 2

[31] I. Rakkolainen, E. Freeman, A. Sand, R. Raisamo, and S. Brewster. A survey of mid-air ultrasound haptics and its applications. *IEEE Transactions on Haptics*, 14(1):2–19, 2020. 2

[32] C. Spearman. The proof and measurement of association between two things. 1961. 6

[33] P. L. Strandholt, O. A. Dogaru, N. C. Nilsson, R. Nordahl, and S. Serafin. Knock on wood: Combining redirected touching and physical props for tool-based interaction in virtual reality. In *Proceedings of the 2020 CHI Conference on Human Factors in Computing Systems*, pp. 1–13, 2020. 3

[34] R. Suzuki, H. Hedayati, C. Zheng, J. L. Bohn, D. Szafir, E. Y.-L. Do, M. D. Gross, and D. Leithinger. Roomshift: Room-scale dynamic haptics for vr with furniture-moving swarm robots. In *Proceedings of the 2020 CHI conference on human factors in computing systems*, pp. 1–11, 2020. 2

[35] R. Suzuki, E. Ofek, M. Sinclair, D. Leithinger, and M. Gonzalez-Franco. Hapticbots: Distributed encountered-type haptics for vr with multiple shape-changing mobile robots. In *The 34th Annual ACM Symposium on User Interface Software and Technology*, pp. 1269–1281, 2021. 2

[36] P. Virtanen, R. Gommers, T. E. Oliphant, M. Haberland, T. Reddy, D. Cournapeau, E. Burovski, P. Peterson, W. Weckesser, J. Bright, S. J. van der Walt, M. Brett, J. Wilson, K. J. Millman, N. Mayorov, A. R. J. Nelson, E. Jones, R. Kern, E. Larson, C. Carey, I. Polat, Y. Feng, E. W. Moore, J. VanderPlas, D. Laxalde, J. Perktold, R. Cimrman, I. Henriksen, E. A. Quintero, C. R. Harris, A. M. Archibald, A. H. Ribeiro, F. Pedregosa, P. van Mulbregt, and contributors. *SciPy: Open source scientific tools for Python*. SciPy Developers, 2020. 6

[37] Y. Weiss, S. Villa, A. Schmidt, S. Mayer, and F. Müller. Using pseudo-stiffness to enrich the haptic experience in virtual reality. In *Proceedings of the 2023 CHI Conference on Human Factors in Computing Systems*, pp. 1–15, 2023. 3

[38] F. Wilcoxon. Individual comparisons by ranking methods. In *Breakthroughs in Statistics: Methodology and Distribution*, pp. 196–202. Springer, 1992. 6

[39] R. S. Witte and J. S. Witte. *Statistics*. John Wiley & Sons, 2017. 8

[40] Y. Zhao and S. Follmer. A functional optimization based approach for continuous 3d retargeted touch of arbitrary, complex boundaries in haptic virtual reality. In *Proceedings of the 2018 CHI Conference on Human Factors in Computing Systems*, pp. 1–12, 2018. 3

[41] Y. Zhou and V. Popescu. Tapping with a handheld stick in vr: Redirection detection thresholds for passive haptic feedback. In *2022 IEEE Conference on Virtual Reality and 3D User Interfaces (VR)*, pp. 83–92. IEEE, 2022. 1

[42] Y. Zhou and V. Popescu. Dynamic redirection for vr haptics with a handheld stick. *IEEE Transactions on Visualization and Computer Graphics*, 29(5):2753–2762, 2023. 1, 3, 4, 5

[43] Y. Zhou and V. Popescu. Detectability of ethd position and speed redirection for vr haptics. In *2024 IEEE International Symposium on Mixed and Augmented Reality (ISMAR)*, pp. 140–149. IEEE, 2024. 5